Proceedings of the International Pipeline Conference & Exposition
IPC2016
September 26-30, 2016, Calgary, Alberta, Canada

IPC2016-64563

A FINITE ELEMENT PROCEDURE TO MODEL THE EFFECT OF HYDROSTATIC TESTING ON SUBSEQUENT FATIGUE CRACK GROWTH

Ted L. Anderson
Team Industrial Services, Inc.
Boulder, Colorado, USA

Greg V. Thorwald
Quest Integrity Group
Boulder, Colorado, USA

ABSTRACT

Hydrostatic testing of pipelines that are subject to pressure cycling and fatigue damage can alter the intrinsic characteristics of flaws that survive the test. The effect is generally favorable, as test pressures well above the maximum operating pressure (MOP) can significantly reduce the subsequent rate of fatigue crack growth. The phenomenon is known as *fatigue retardation*, which is caused by crack closure due to compressive residual stresses created by plastic deformation during the hydrotest.

Fatigue retardation following an overload event is a well-known phenomenon in metallic structures, but there has been little or no effort to take advantage of this beneficial effect in pipelines. This paper presents a modeling procedure aimed at quantifying fatigue retardation following a hydrostatic test. A series of 3D elastic-plastic finite element simulations have been performed to model fatigue crack growth following a pressure test. The effect of test pressure and MOP on plasticity-induced crack closure was studied. The relative effect of fatigue retardation on remaining life was demonstrated with several examples. In some cases, the results were counter intuitive.

BACKGROUND

Hydrostatic testing is a well-established integrity management tool for pipelines, both as an initial quality control check at the time of construction, as well as a means to demonstrate fitness for continued service after years of operation. The basic logic of hydrostatic testing is as follows: subjecting a pipeline to test pressures well above the maximum operating pressure (MOP) identifies and removes the most severe flaws from the line and ensures that remaining flaws are below the critical size at the test pressure. When the pipeline is returned to service, flaws that survive the hydrostatic test are well below the critical size at the MOP. If the line is subject to pressure cycling, these flaws may grow by fatigue and will eventually lead to failure if no corrective action is taken. A pressure cycle fatigue analysis (PCFA) is typically performed to estimate the remaining life of the line following a hydrostatic test. A follow-up hydrostatic test or inline inspection can then be scheduled based on the results of a PCFA.

Traditional PCFA models predict that remaining life following a hydrostatic test increases with test pressure. A higher test pressures corresponds to a smaller critical flaw size. The PCFA uses the critical flaw size at the test pressure as the starting point in the life assessment. Smaller initial flaws take more time to grow to failure; hence the direct relationship between test pressure and the estimated life of the pipeline.

These models ignore the fact that crack-like flaws are modified by hydrostatic testing. A test pressure that is significantly above the MOP leads to plastic deformation at the tip of a flaw, which results in a zone of compressive residual stresses. Upon subsequent pressure cycling, the rate of fatigue crack propagation is reduced relative to what it would have been in the absence of the pressure test. This effect is beneficial, as it extends the life of the pipeline. This is a well-known phenomenon called *fatigue retardation*, which affects all metallic structures subject to cyclic loading and overload events.

The consensus among fatigue experts is that retardation is caused by *crack closure*, where compressive residual stress forces the crack faces to close, even in the presence of a positive applied load (1, 2). Figure 1 illustrates the phenomenon of crack closure following an overload. Prior to the overload event, crack-tip plasticity resulting from normal operating loads produces a plastic wake on the crack faces, which generates compressive residual stress that can lead to

closure in some circumstances. An overload event generates a large plastic zone, which creates larger compressive residual stress than in the plastic wake. Consequently, crack closure may occur when the crack grows into the overload zone.

When crack closure occurs during pressure cycling, the effective magnitude of cyclic pressure decreases, which results in a reduction in crack growth rate. This leads to a longer life, as the right side of Fig. 1 illustrates. Figure 2 is a plot of fatigue crack growth data, which was obtained for a carbon steel with properties consistent with the API 5L-X46 grade. In this experiment, the specimen was cycled between zero and a nominal stress equal to 50% of yield. A single load spike to 100% of yield was applied, after which the previous constant-amplitude loading was resumed. The crack growth rate dropped significantly after the overload event, but it eventually recovered to a nominal rate (unaffected by closure) when the crack grew through the overload zone.

This article presents a methodology to extend standard PCFA models to include retardation and closure effects. Three-dimensional elastic-plastic finite element simulation was used to model the effect of a pressure spike on plastic deformation in front of a crack, as well as the development of compressive residual stresses that result in crack closure. The finite element results were then used in several PCFA examples that illustrate the relative impact of crack closure on remaining life.

FINITE ELEMENT METHODOLOGY

Figure 3 shows the finite element model used in the present study. A 12-inch diameter pipe with 0.25-inch wall was modeled. The model included a 4-inch long by 0.0625-inch deep (25% wall) longitudinal surface crack on the OD. The finite element model in Fig. 3 is ¼-symmetric with a rigid contact surface on the crack face to capture closure effects.

The finite element model was created with the FEACrack software (3), a commercial pre- and post-processor developed by Quest Integrity for 3D crack analysis. A special "cell-type" mesh was implemented in order to growth the crack by node release. The element size at the crack tip, and therefore the crack growth increment, was 0.005 in. The WARP3D nonlinear finite solver (4), which was developed by the University of Illinois, was used for all simulations because it incorporates crack growth by node release at user-specified time steps.

The finite element model was subjected to a range of pressure cycle scenarios combined with crack propagation. Table 1 lists the eight load cases considered. The hydrostatic test pressure ranged from 90 to 105% of specified minimum yield strength (SMYS), and was preceded and followed by constant-amplitude loading from zero to the MOP, which was taken as either 72% or 50% of SMYS.

Figure 4 shows the loading history for the case where MOP = 50% SMYS and the test pressure = 100% SMYS. Each increment of crack growth was preceded by 4 loading cycles in order to establish the plastic zone at a given crack size. The analysis included a total of 20 crack advances of 0.005-in each, 2 of which occurred before the pressure spike and the remainder following the spike. Each loading cycle in the simulation was applied over numerous time steps. The load history plotted in Fig. 5 entailed nearly 9,000 time steps.

The purpose of the loading history in Fig. 5 as well as the other cases listed in Table 1 was to grow the crack through a zone of compressive residual stress created by the pressure spike. This approach enabled the authors to evaluate the effect of pressure cycling and hydrostatic testing on the crack closure behavior, which in turn influences remaining life.

TABLE 1.
Load Cases Considered in the Present Study

MOP, %SMYS	Hydrostatic Test Pressure, %SMYS			
	90	95	100	105
72	●	●	●	●
50	●	●	●	●

FINITE ELEMENT RESULTS

The load histories listed in Table 1 produced a range of crack closure behavior in the finite element simulations. Crack closure can be detected by a number of means, including changes in load-displacement behavior. In the present study, pressure was plotted versus the displacement of a node at the center of the crack length on the OD surface. This approach is equivalent to using a clip gage at the crack mouth in an experiment. Figure 5 schematically illustrates the effect of closure on the pressure versus crack opening displacement in a given cycle. Under purely linear elastic conditions, the load and unload portions of the cycle fall on a single straight line with a slope that is a function of the crack depth. In the present study, the MOP was sufficiently high to cause yielding at the crack tip, which resulted in a closed pressure-displacement loop. When the crack faces contact upon unloading from MOP, the slope of the pressure-displacement curve changes abruptly, as Fig. 5(b) illustrates.

Figure 6 is a plot of finite element results for the load case where MOP = 50% SMYS and the pressure spike = 100% SMYS. The slope of the pressure versus crack opening displacement curve is plotted for the unloading portion of the cycle. The family of curves corresponds to various crack depths, where pressure/displacement slope decreases with crack growth. The top curve in Fig. 6 is the pressure/displacement slope immediately after the pressure spike. No closure occurs at this point. With subsequent crack growth (curves shifting downward), closure is observed, as evidenced by abrupt changes in slope. Upon further crack growth, closure effects gradually disappear.

Figure 7 is a plot of opening stress, defined at the minimum stress level where the crack is fully open, versus crack propagation distance for MOP = 72% SMYS. A high opening stress indicates significant closure effects. The maximum impact of closure occurs when the crack propagates a short

distance (0.010-0.015 in) into the overload zone. The largest opening stress values were achieved when the pressure spike was 90 to 95% SMYS, and the lowest closure stress levels were observed following a test pressure of 105% SMYS.

Figure 8 compares the opening stress for MOP = 72% and 50% SMYS. Given the same hydrostatic test pressure, greater closure effects are observed at the lower MOP. Figure 9 illustrates the reason for this trend. The hydrostatic test results in significant crack blunting and a zone of compressive residual stress in front of the crack. After a finite amount of crack growth beyond the overload event, the crack tip opening displacement (CTOD) is governed by the operating pressure. If the pipe is unloaded from the MOP (72% and 50% of yield in Cases 1 and 2, respectively) to 20% of yield, closure is observed in Case 2 but not in Case 1 (see Fig. 8). In order for closure to occur at or above σ_{min}, the compressive residual stresses due to the overload must overcome the crack blunting that occurs at σ_{max}. The size of the overload plastic zone and the magnitude of the compressive residual stresses are governed by the overload event, but the opening stress is also influenced by crack blunting in subsequent cycles.

LIFE PREDICTION EXAMPLES

A series of pressure cycle fatigue analyses have been performed to demonstrate the relative effect of fatigue retardation from crack closure. The PRCI MAT-8 model (5) was used to compute critical flaw sizes at a range of hydrostatic test pressures. The calculated remaining life corresponds to the estimated time for a critical flaw at the test pressure to grow to failure at the MOP. Actual pressure cycle data from a crude oil pipeline were used for the PCFA. Crack closure was taken into account by reducing the effective cyclic stress when the hoop stress dropped below the opening stress (Figs. 7 and 8). The analysis assumed a fracture toughness of 200 ksi√in and a starting flaw length of 4 in.

The results of the fatigue analyses are plotted in Figs. 10 to 12. Figure 10 shows results pertaining to pressure cycling at a pumping station discharge, designated as Station X for the purpose of identification in this paper. The MOP = 72% SMYS in this case. The retardation model has little impact on the predicted lives because there are few low-pressure excursions at the discharge to Station X. Fatigue retardation is the result of crack closure, which occurs only when pressure drops below the opening pressure. Figure 11, which corresponds to the suction of the pumping station downstream of Station X, shows a more significant impact of fatigue retardation. In this case, there are more frequent low-pressure excursions. Note that the life versus hydrostatic test pressure curve that includes retardation is flatter than the other curve because retardation effect are more pronounced for test pressures below 100% SMYS

Figure 12 corresponds to a hypothetical pressure history that was obtained by capping the suction pressure data (Fig. 11) at 50% SMYS. The unaltered pressure data for the pumping station suction location actually seldom exceeded 50% SMYS, so capping the pressure had little effect on cyclic loading. However, reducing MOP from 72% to 50% SMYS prolongs the life for two reasons:

1. The critical flaw size increases when MOP decreases, so additional fatigue crack growth precedes failure.
2. The magnitude of crack closure and the resulting retardation are a function of the ratio of the test pressure to MOP, as Figs. 8 and 9 illustrate. Decreasing MOP results in greater retardation in crack growth, given the same hydrostatic test pressure.

The upper curve in Fig. 12 indicates that fatigue life actually *decreases* when test pressure exceeds 95% SMYS because fatigue retardation effects, which exhibit a decreasing trend with test pressure (see below), overwhelms other factors. Consequently, there is little or no value in higher test pressures in this case, particularly since remediation costs will increase with test pressure due to hydrotest failures.

Figure 13 is a plot of the ratio of calculated fatigue lives with and without retardation effects incorporated into the PCFA. The relative impact of retardation decreases with test pressure in all cases considered. This trend can be explained in terms of the mechanism for formation of compressive residual stresses at the crack tip following a pressure test. The highest residual stresses are generated when the plastic zone created during the overload event is contained within material that is stressed in the elastic range. When the test pressure is removed, the elastically deformed material recovers its original shape, which compresses the overload zone. When the entire cross section in front of the crack deforms plastically, the relative magnitude of the compressive forces exerted on the overload zone is less.

Finally, one should not focus on the *absolute* magnitude of the fatigue lives shown in Figs. 10 to 12. These life calculations were based on a particular set of assumptions on material properties and crack aspect ratio. The purpose of Figs. 10 to 12 is to demonstrate the *relative* impact of test pressure, with and without fatigue retardation effects taken into account

CONCLUDING REMARKS

This study represents an initial attempt to quantify the degree to which hydrostatic testing changes the intrinsic properties of flaws that survive the test. Further work is necessary to refine and extend the retardation model introduced in this paper. Of course, experimental validation and benchmarking is also required.

Fatigue retardation is a beneficial phenomenon, as it prolongs life, so it is desirable to understand and quantify this effect. Moreover, accounting for fatigue retardation may lead to life predictions that are counter intuitive. Figure 13, for example, shows that remaining life may actually decline with increasing test pressure in some circumstances. The conventional wisdom in the pipeline industry on hydrostatic test pressure is that *higher is better* with respect to remaining life. A more complete understanding of the science of hydrostatic testing may contradict the conventional wisdom.

This project is part of a larger effort to develop predictive models for hydrostatic testing (6). The goal of this research is to provide the industry with tools that enable operators to optimize hydrostatic testing procedures, both in terms of pipeline integrity and economic benefit.

ACKNOWLEDGMENTS

The authors wish to acknowledge the support of Koch Pipeline LLP and ExxonMobil Research and Engineering. Prior to the present study, NASA Marshall Space Flight Center provided funding to enhance the WARP3D and FEACrack software to enable user-driven crack front node release.

REFERENCES

1. Anderson, T.L., *Fracture Mechanics: Fundamentals and Applications*. 3rd Edition, Taylor & Francis, Boca Raton, FL, 2005.
2. Newman, J.C., "Prediction of Fatigue Crack Growth under Variable Amplitude and Spectrum Loading Using a Closure Model." ASTM STP 761, American Society for Testing and Materials, Philadelphia, 1982, pp. 255-277.
3. FEACrack, Version 3.2.27, Quest Integrity Group, 2015.
4. WARP3D-Release 17.5.8: 3-D Dynamic Nonlinear Fracture Analyses of Solids Using Parallel Computers, February 9, 2015.
5. Anderson, T.L., "Development of a Modern Assessment Method for Longitudinal Seam Weld Cracks." Pipeline Research Council Inc., Catalog No. PR-460-134401, 2016.
6. Anderson, T.L., "A Predictive Model for Optimizing Hydrostatic Test Pressures in Seam-Welded Pipelines." Pipeline Pigging and Integrity Management Conference, Houston, TX, February 10-11, 2016.

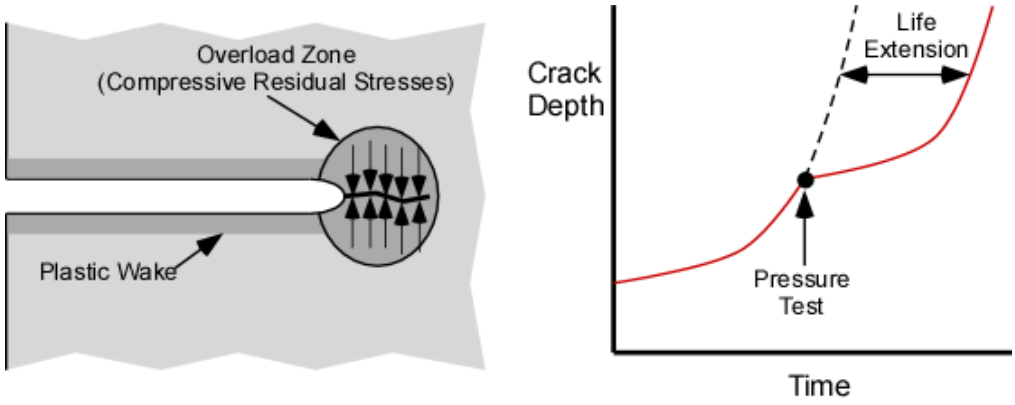

FIGURE 1. Crack closure mechanism for fatigue retardation following a pressure test. The overload generates a zone of compressive residual stresses at the crack tip, which results in slower fatigue crack propagation due to crack closure.

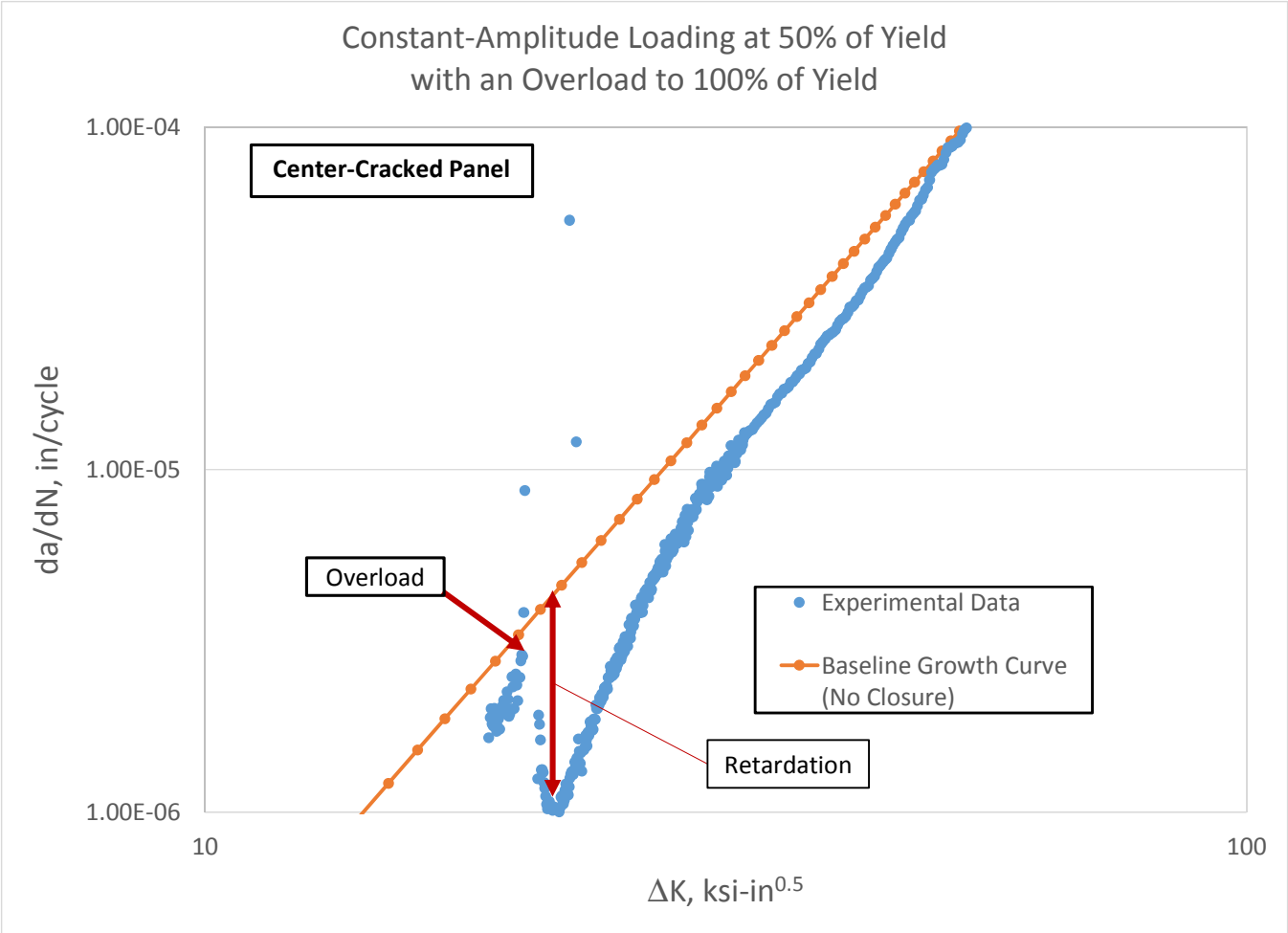

FIGURE 2. Fatigue crack growth data for a carbon steel equivalent to API 5L-X46.

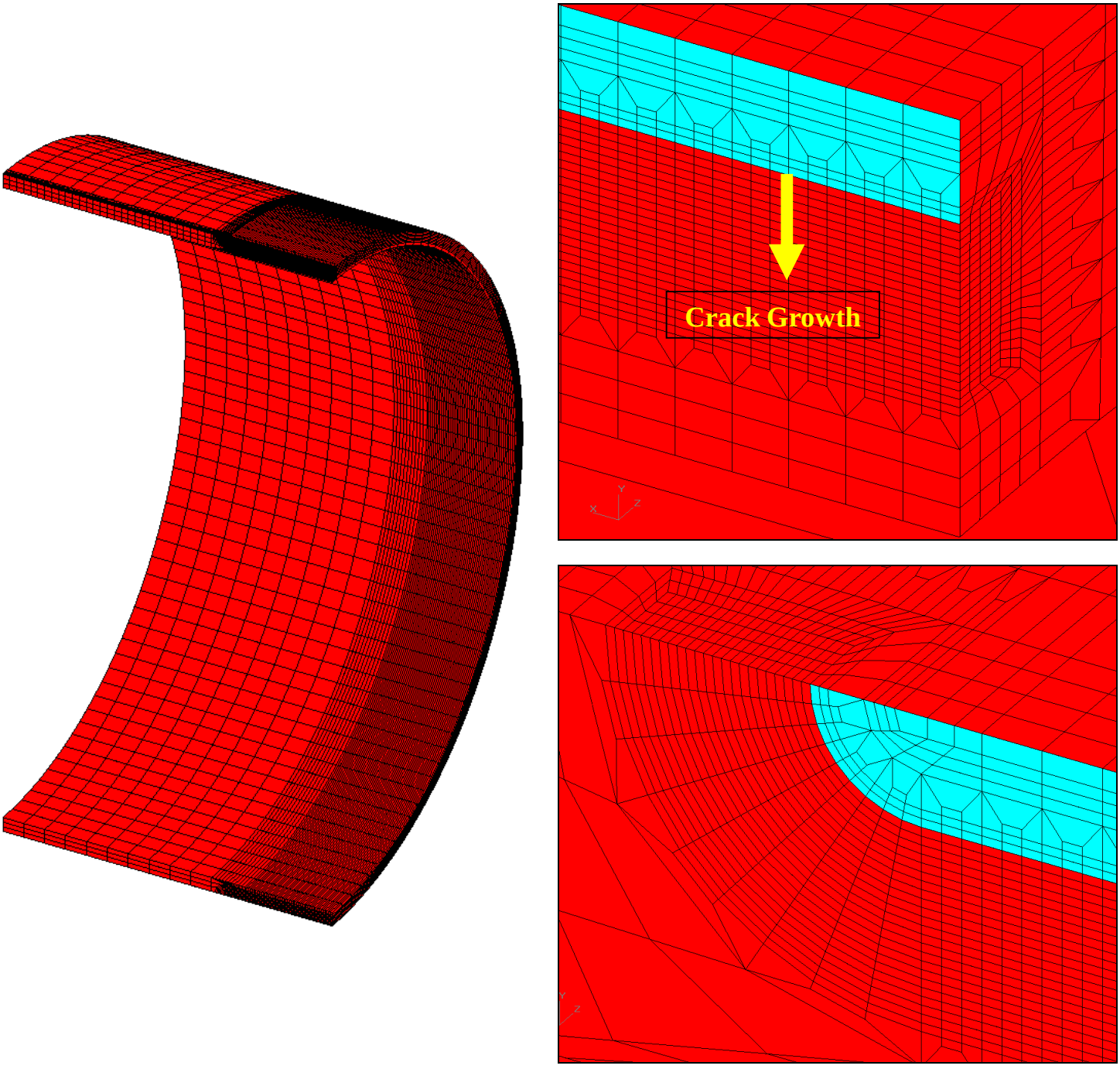

FIGURE 3. Quarter-symmetric finite element model to simulate fatigue retardation.

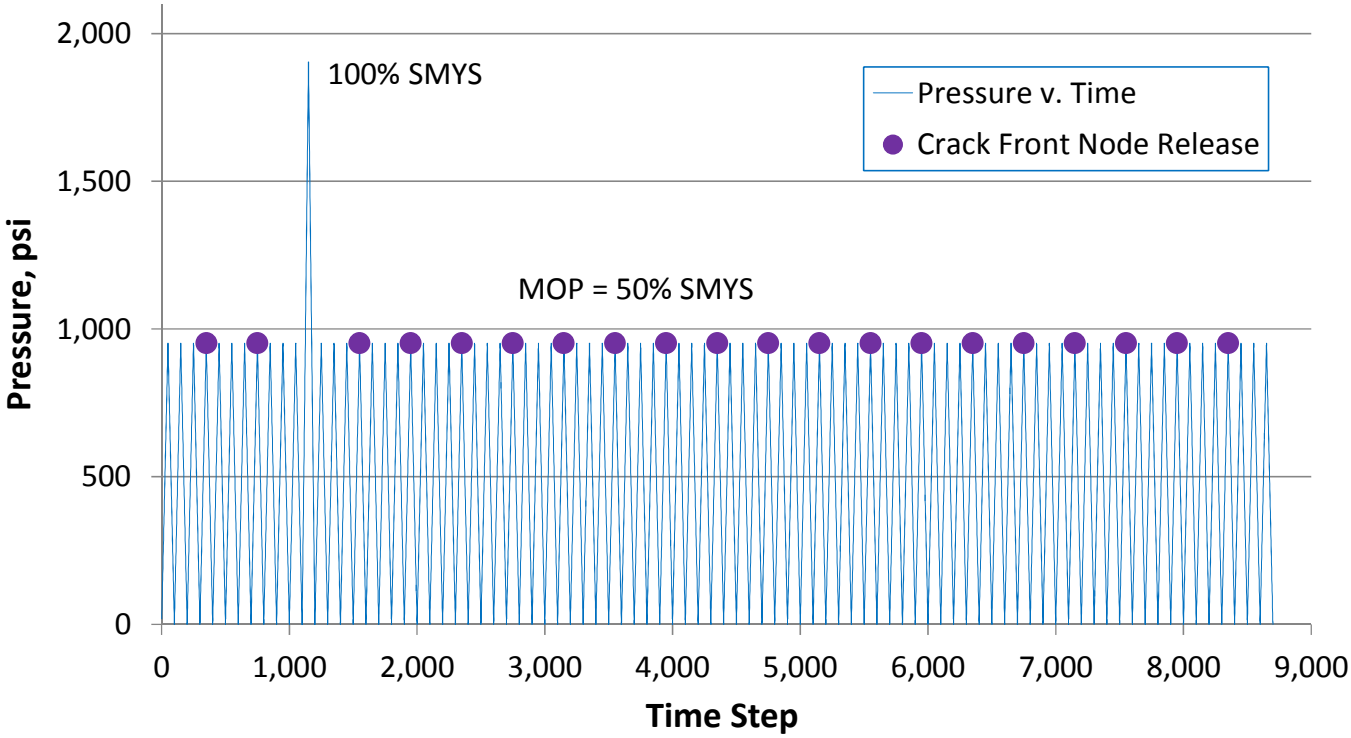

FIGURE 4. Load history for a typical finite element simulation. A pressure spike to 100% SMYS was preceded and followed by constant amplitude cycling between 0 and 50% SMYS in this example.

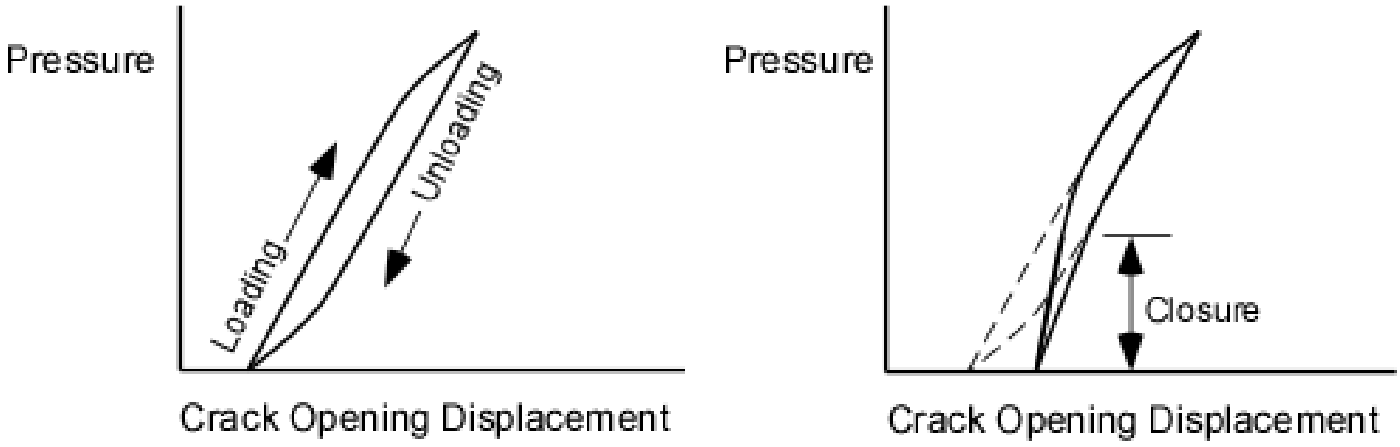

(a) No crack closure.

(b) With crack closure.

FIGURE 5. Schematic illustration of a pressure cycle with and without crack closure.

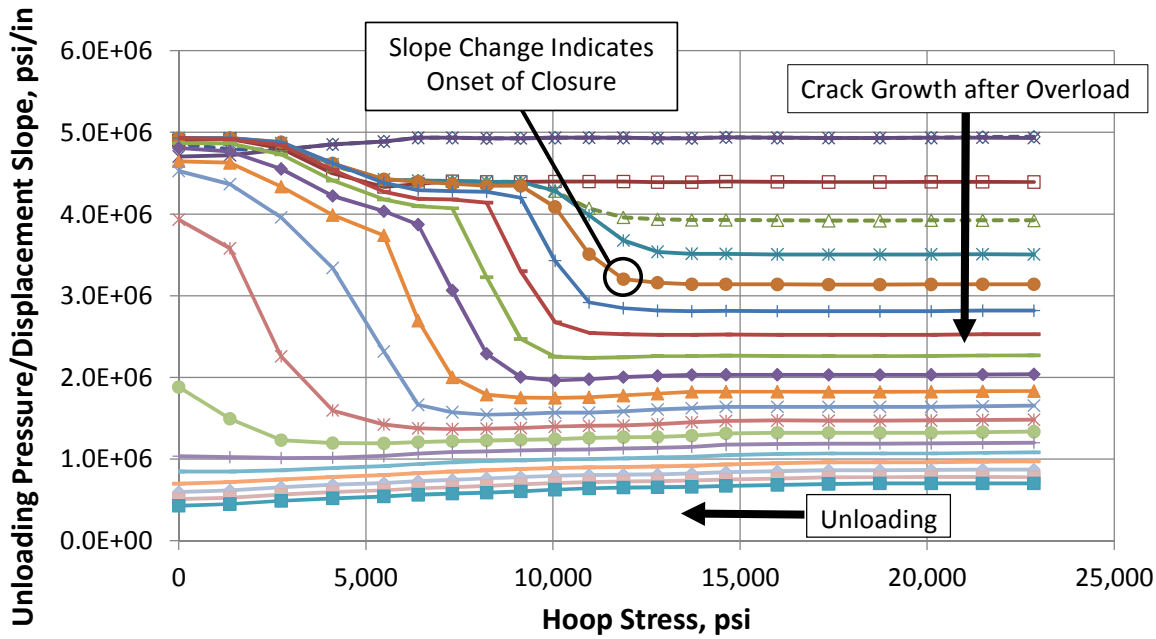

FIGURE 6. Unloading pressure/crack opening displacement slope at various crack sizes following a hydrostatic test to 100% SMYS.

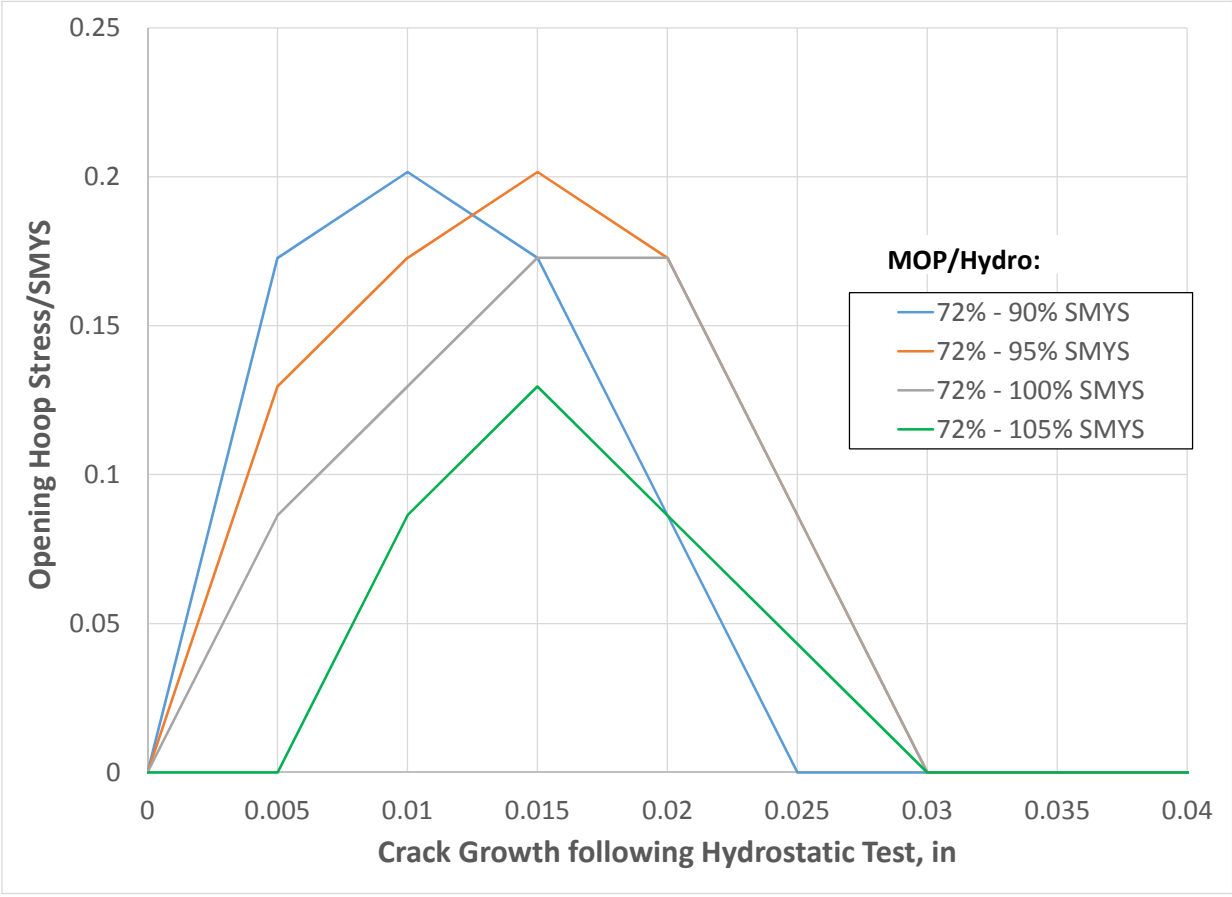

FIGURE 7. Crack opening stress following a hydrostatic test.

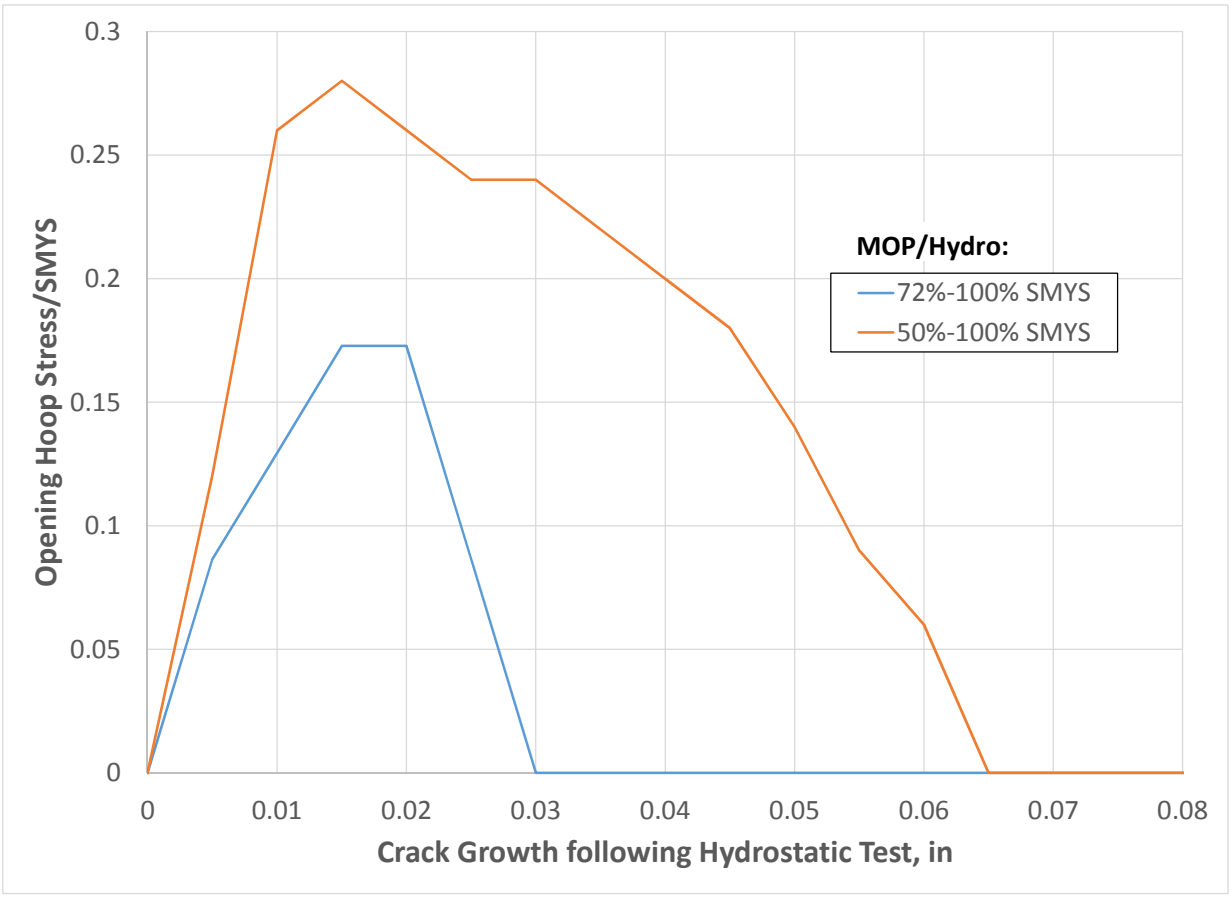

FIGURE 8. Effect of MOP following a hydrostatic test on crack closure behavior.

Case 1: $\sigma_{max} = 0.72\ \sigma_{YS}$ and $\sigma_{min} = 0.2\ \sigma_{YS}$

Case 2: $\sigma_{max} = 0.50\ \sigma_{YS}$ and $\sigma_{min} = 0.2\ \sigma_{YS}$

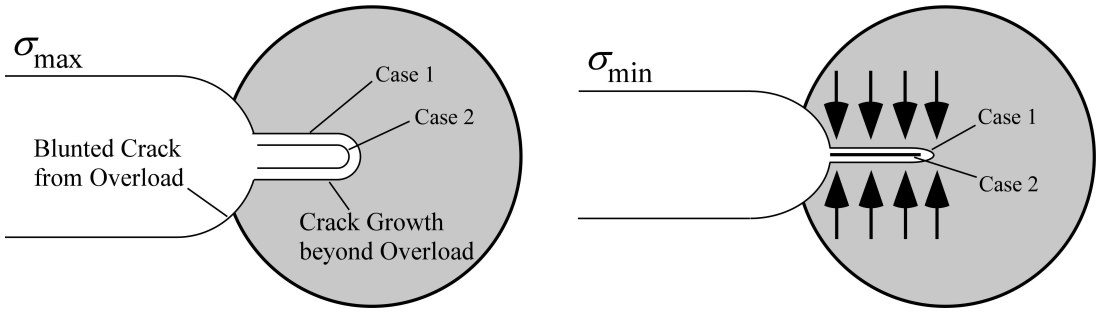

FIGURE 9. Crack propagation following an overload. In order for closure to occur at or above σ_{min}, compressive residual stresses must overcome crack blunting at σ_{max}. Consequently, crack closure behavior is a function of the magnitude of both the overload and the subsequent maximum stress.

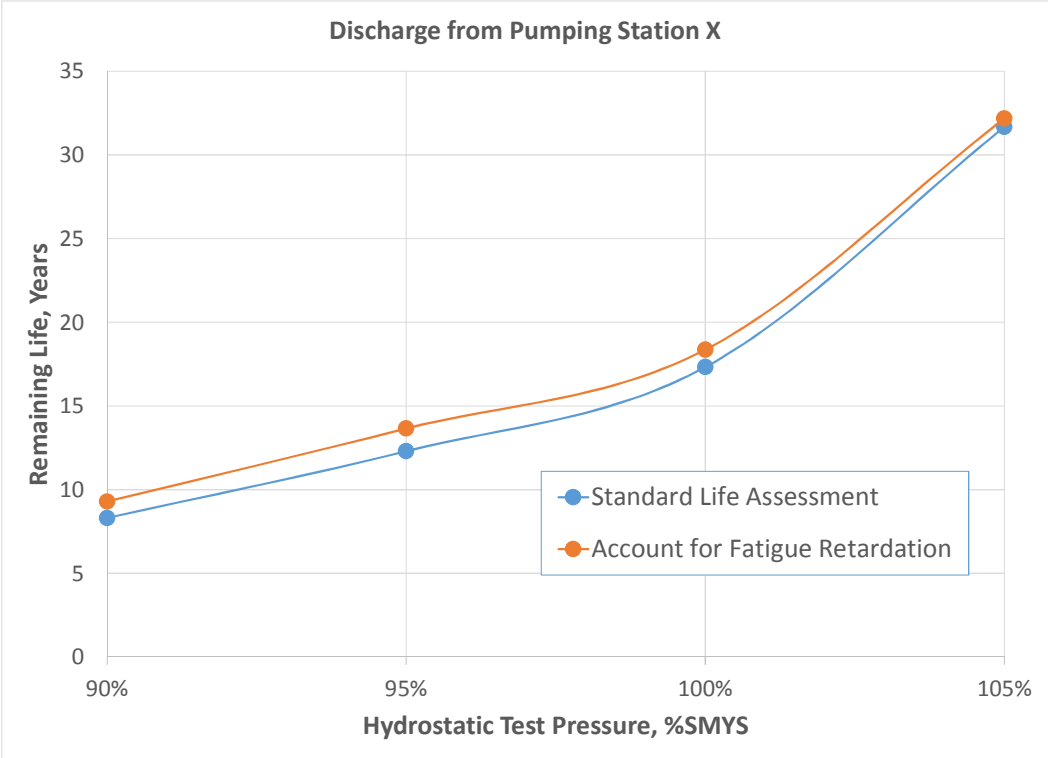

FIGURE 10. Effect of fatigue retardation on remaining life at a pumping station discharge.

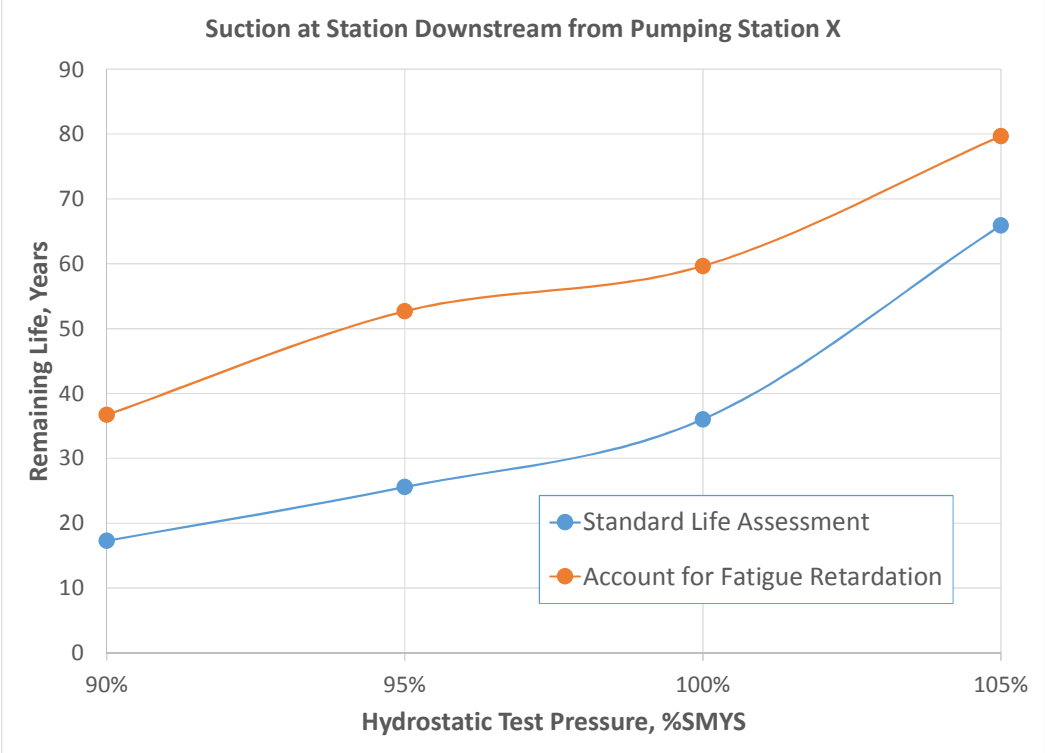

FIGURE 11. Same as Fig. 10, but at the suction of the pumping station downstream from Station X.

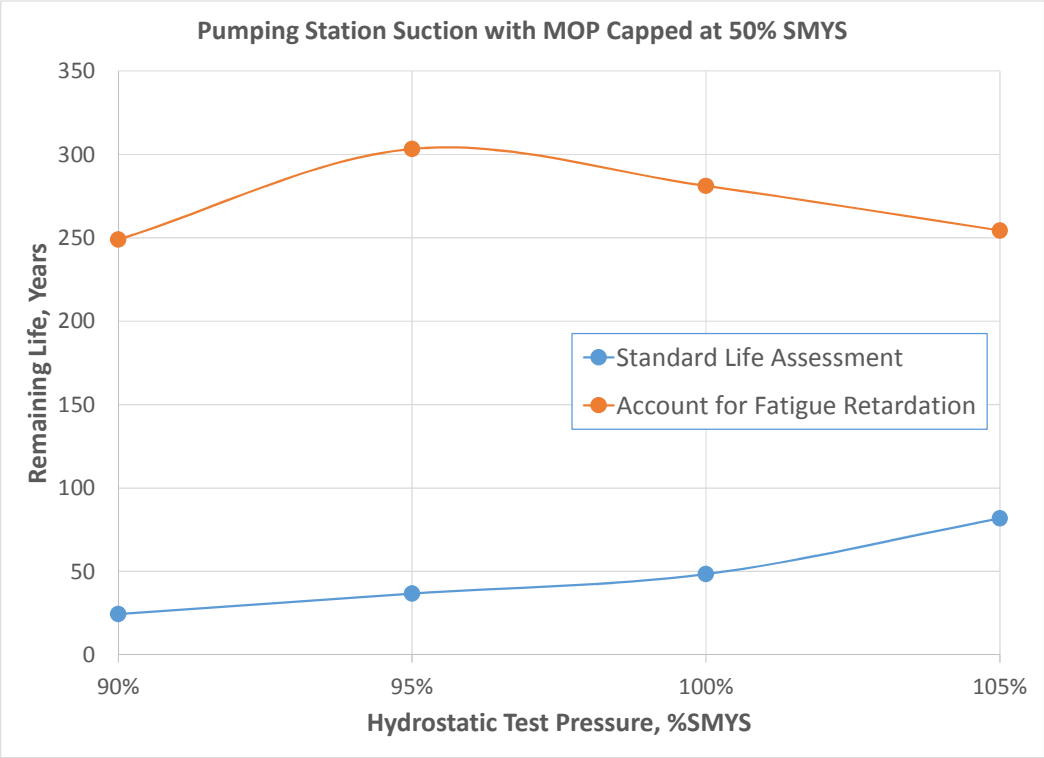

FIGURE 12. Same as Fig. 11, but with MOP capped at 50% SMYS.

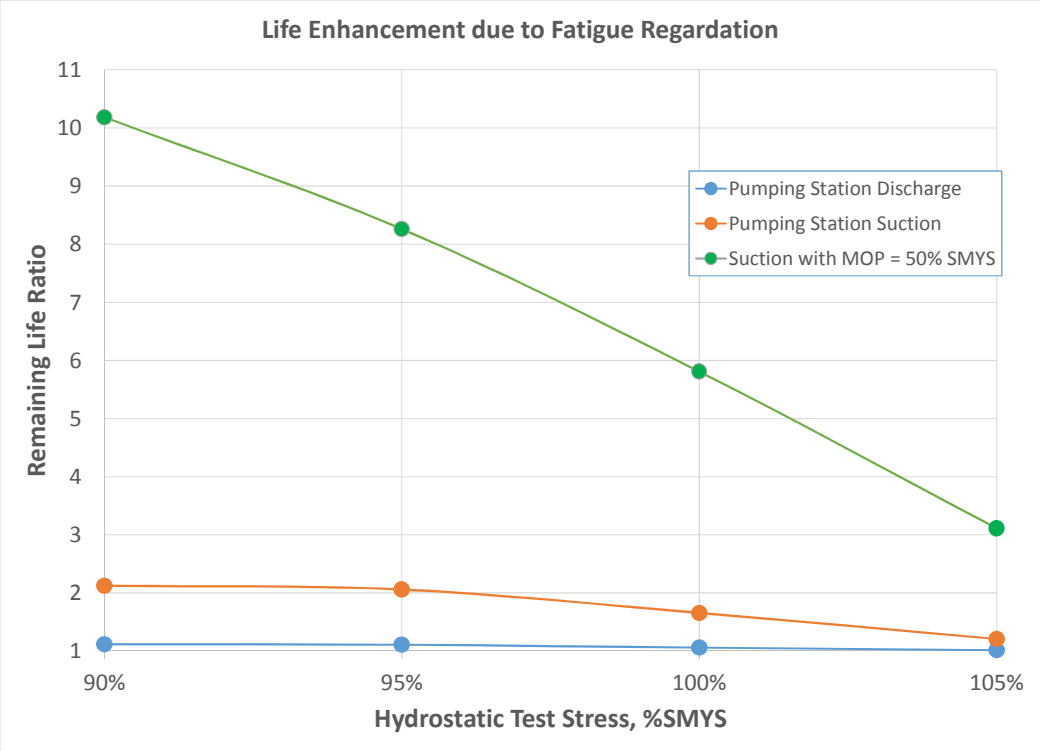

FIGURE 13. Ratio of life estimates with and without including retardation effects